



Subpolar Mode Water in the northeastern Atlantic:

1. Averaged properties and mean circulation

Elena Brambilla¹ and Lynne D. Talley¹

Received 19 December 2006; revised 9 August 2007; accepted 6 November 2007; published 23 April 2008.

[1] Subpolar Mode Waters (SPMW) in the eastern North Atlantic subpolar gyre are investigated with hydrographic and Lagrangian data (surface drifters and isopycnal floats). Historical hydrographic data show that SPMWs are surface water masses with nearly uniform properties, confined between the ocean surface and the permanent pycnocline. SPMWs represented by densities $27.3\sigma_\theta$, $27.4\sigma_\theta$, and $27.5\sigma_\theta$ are present in the eastern subpolar gyre and are influenced by the topography and the regional circulation. Construction of an absolute surface stream function from surface drifters shows that SPMWs are found along the mean path of each of the several branches of the North Atlantic Current (NAC) and their density increases gradually downstream. The Rockall Trough branch of the NAC carries $27.3\sigma_\theta$, $27.4\sigma_\theta$, and $27.5\sigma_\theta$ SPMW toward the Iceland-Faroe Front. In the Iceland Basin, the Subarctic Front along the western flank of the Rockall Plateau carries a similar sequence of SPMW. The western side of the Central Iceland Basin branch of the NAC, on the other hand, veers westward and joins the East Reykjanes Ridge Current, feeding the $27.5\sigma_\theta$ SPMW on the Reykjanes Ridge. The separation among the various NAC branches most likely explains the different properties that characterize the $27.5\sigma_\theta$ SPMW found on the Reykjanes Ridge and on the Iceland-Faroe Ridge. Since the branches of the NAC have a dominant northeastward direction, the newly observed distribution of SPMW combined with the new stream function calculation modify the original hypothesis of McCartney and Talley (1982) of a smooth cyclonic pathway for SPMW advection and density increase around the subpolar gyre.

Citation: Brambilla, E., and L. D. Talley (2008), Subpolar Mode Water in the northeastern Atlantic: 1. Averaged properties and mean circulation, *J. Geophys. Res.*, 113, C04025, doi:10.1029/2006JC004062.

1. Introduction

[2] Subpolar Mode Waters are the near-surface water masses of the subpolar North Atlantic characterized by thick layers of nearly uniform properties (temperature, salinity, density) [McCartney and Talley, 1982]. Masuzawa [1969] first defined mode waters in the context of the North Pacific Subtropical Mode Water with its large volume of water with nearly uniform temperature of 16° – 18°C . “Mode Water” is now broadly used to describe a large number of water masses with nearly uniform properties (density, temperature, salinity) [Hanawa and Talley, 2001]. The original description of SPMW by McCartney and Talley [1982] has been partially revised by more recent studies [e.g., Talley, 1999; Read, 2001]. Here and in an accompanying paper [Brambilla et al., 2008], we present a new analysis of SPMW in the northeastern Atlantic, highlighting the link between the averaged SPMW location and properties and the predominantly northeastward mean circulation of the region. The most significant addition to the

earlier studies is an analysis of the circulation, using Lagrangian data in conjunction with hydrographic data.

[3] SPMWs have long been the object of particular attention due to their important role in the transfer of warm and salty North Atlantic water from the subtropical gyre to the Nordic Seas and Labrador Sea. McCartney and Talley [1982], in their original description of SPMWs, suggested that SPMWs, formed during late winter convection, follow the cyclonic circulation of the subpolar gyre, gradually increasing their density owing to buoyancy loss caused by cooling along the path. The final products of this gradual transformation are the Labrador Sea Water and the dense water masses formed in the Nordic Seas. Thus SPMWs are the water masses that participate in the upper flow of the overturning circulation and provide much of the water that is eventually transformed into the several components of North Atlantic Deep Water (NADW) [e.g., McCartney and Talley, 1982, 1984; Schmitz and McCartney, 1993; McCartney and Mauritzen, 2001].

[4] The interest in SPMW studies is also driven by the possible role of these particular water masses in feedback between the subpolar gyre and the atmosphere [Hanawa and Talley, 2001]. Because of their large volume and their nearly uniform temperature, mode waters represent in general a near-surface reservoir of heat that is slowly

¹Scripps Institution of Oceanography, University of California, San Diego, La Jolla, California, USA.

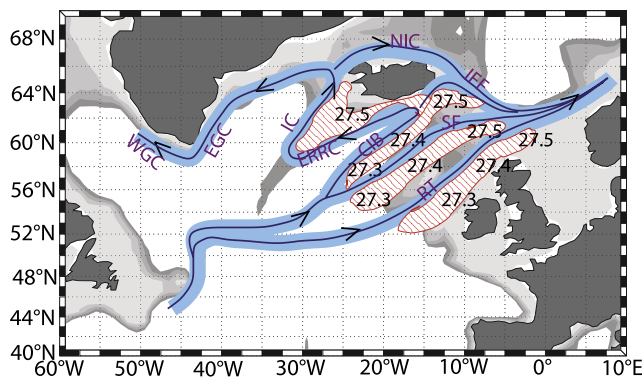


Figure 1. Schematic of the mean currents (light blue) in the subpolar gyre and the SPMWs (red) associated with them. The density sequence in each SPMW patch is indicated. The darker lines represent the current fronts. The currents are as follows: RT, Rockall Trough Branch of the NAC; SF, Subarctic Front; CIB, Central Iceland Basin Branch of the NAC; ERRC, East Reykjanes Ridge Current; IC, Irminger Current; NIC, North Iceland Current; IFF, Iceland Faroe Front; EGC, East Greenland Current; WGC, West Greenland Current.

released back to the atmosphere and might influence the global atmospheric circulation [Kwon and Riser, 2004].

[5] Schmitz and McCartney [1993] synthesized prior North Atlantic transport studies, reporting that SPMW is transported at a rate of 5 Sv ($1 \text{ Sv} = 10^6 \text{ m}^3 \text{ s}^{-1}$) into the Nordic Seas across the Iceland-Faroe Ridge and the Denmark Strait. In addition, 7 Sv of dense water sinks in the Labrador Sea that is replenished by the SPMW from the subpolar gyre. Bersch [1995], calculating the volume transport across a hydrographic section (WOCE A1/AR7E) from Cape Farvel (southern tip of Greenland) to Porcupine Bank (offshore of Ireland), computed a similar balance between the SPMW that circulates in the upper layer of the subpolar gyre and the LSW formed in the Labrador Sea.

[6] In these prior studies of SPMW, it has been assumed that the SPMWs that enter the Nordic Seas and the Labrador Sea are branches of the same cyclonic circulation in the subpolar gyre. Talley [1999], on the other hand, questioned the concept of a complete cyclonic flow of SPMWs around the subpolar gyre feeding the LSW. The Subarctic Front flows northward east of Iceland, feeding the Iceland-Faroe Front and the Norwegian Current [e.g., Flatau et al., 2003]. SPMWs east of the Subarctic Front do not appear to connect to SPMWs west of the front. The lighter SPMWs are located in the southeastern part of the basin (Rockall Trough) where the surface circulation is directed northeastward, connecting the Atlantic water to the Norwegian Current [Orvik and Niiler, 2002; Orvik and Skagseth, 2003], hence making difficult the link between this mode water and denser ones on the Reykjanes Ridge [Perez-Brunius et al., 2004]. On the other hand, at subsurface depths, the circulation is cyclonic on shoaling isopycnals [Bower et al., 2002], possibly permitting a connection between water from the Subarctic Front and the denser SPMW on the Reykjanes Ridge (M. S. McCartney, personal communication, 2006).

[7] Read [2001] identified SPMWs in the eastern subpolar gyre from hydrographic data collected during the CON-

VEX-91 survey (two hydrographic sections between Greenland and Ireland). Light SPMW was found in the eastern part of the subpolar gyre (Rockall Trough), while denser SPMW was found on the Reykjanes Ridge. These SPMWs are separated horizontally by highly stratified water masses not belonging to any SPMW class, confirming the previous observation by Talley [1999]. Therefore observations along those hydrographic sections do not support the smooth cyclonic progression of SPMW hypothesized by McCartney and Talley [1982].

[8] This and the accompanying paper [Brambilla et al., 2008] aim to clarify the averaged location and progressive connection of SPMWs. Hydrographic and Lagrangian velocity data are used to map the SPMWs, their properties, relation to the mixed layer, and circulation.

[9] In the northeastern Atlantic (40°W – 0°E , 50°N – 70°N), we confirm that SPMWs are part of the surface layer that roughly extends vertically from the ocean surface to the permanent pycnocline. Thus SPMWs are the water masses through which the shallow circulation carries warm and salty water to the sites of dense water formation [McCartney and Talley, 1982; Talley, 2003].

[10] Since the original analysis of McCartney and Talley [1982], it has become clear that the subpolar circulation consists of several separate intense northeastward currents, the Rockall Trough branch and Iceland Basin branches (Central Iceland Basin branch and Subarctic Front) of the North Atlantic Current (NAC) and the Irminger Current [Fratantoni, 2001; Flatau et al., 2003; Reverdin et al., 2003; Pollard et al., 2004]. Combining the results from hydrographic and Lagrangian data, we show that SPMWs are associated with each of these intense currents (Figure 1) and that they are not connected by a cyclonic flow [McCartney and Talley, 1982].

[11] The paper is organized as follows. Section 2 describes the data used. Section 3 discusses the depth of the SPMWs relative to the depth of the winter mixed layer. In section 4, we detail the characteristics of the SPMWs in the eastern subpolar gyre and the seasonal variation of the location of SPMWs. In section 5, we analyze the circulation of the eastern subpolar gyre using Lagrangian observation to reference the geostrophic flow. In section 6, we summarize the main results of this study.

2. Data

[12] Hydrographic and Lagrangian data sets are used. Historical (1900–1990) hydrographic bottle data from the National Oceanographic Data Center (NODC) (Figure 2) are used to describe the averaged water mass properties (potential density, salinity, potential temperature, depth) and to compute the winter mixed layer depth. Hydrographic data from six World Ocean Circulation Experiment (WOCE) cruises are also used: A16 in July–August 1988, AR12 in September–November 1996, AR24-147 in November–December 1996, A24 in May–July 1997, AR24-154 in October–November 1997, and AR16 in June–August 2003.

[13] The Lagrangian data set includes surface drifters drogued at 15 m to compute the stream function of the currents at the surface, as in work by Niiler et al. [2003], and isopycnal floats targeted on the $27.5\sigma_\theta$ isopycnal to compute the isopycnal stream function, following Bower et

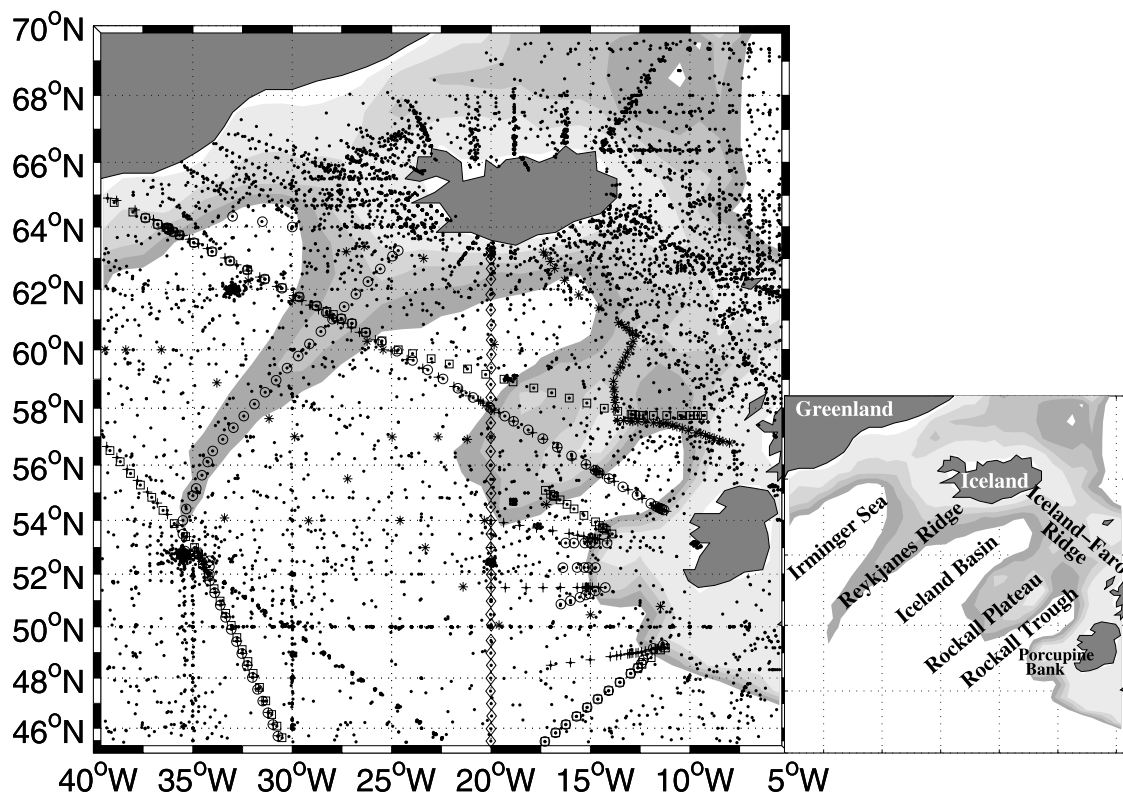


Figure 2. Study area. Topography is shaded; the darkest contour is 2000 m, the lightest is 10 m, contour interval is 500 m. The round dots correspond to the historical hydrographic stations, and the symbols correspond to the WOCE cruises: AR12 1996 September–November (asterisk); AR24-147 1996 November–December (circle); A24 1997 May–July (square); AR24-154 1997 October–November (plus); A16 1988 July–August; and AR16 2003 June–August (diamond). In the insert, we report the names of the topographic features.

al. [2002]. The surface drifters are from the Global Drifter Program at the National Oceanographic and Atmospheric Administration’s (NOAA) Atlantic Oceanographic and Meteorological Laboratory (AOML). They cover the period from 1990 to 2002. These data have been used in several North Atlantic surface circulation studies [Fratantoni, 2001; McClean *et al.*, 2002; Reverdin *et al.*, 2003; Niiler *et al.*, 2003; Flatau *et al.*, 2003; Brambilla and Talley, 2006]. Acoustically tracked isopycnal floats (RAFOS) ballasted for $\sigma_\theta = 27.5 \text{ kg/m}^3$ were deployed as part of the U.S. Atlantic Climate Change Experiment, which was part of WOCE. They cover the period 1996–1997 [Bower *et al.*, 2002] and measured temperature and pressure [Rossby *et al.*, 1986].

[14] Finally, annual mean hydrographic data objectively mapped on a $1^\circ \times 1^\circ$ grid from the World Ocean Atlas 2001 (WOA01) [Conkright *et al.*, 2002] were used to compute the absolute stream function on the $27.3\sigma_\theta$, $27.4\sigma_\theta$ and $27.5\sigma_\theta$ isopycnal surfaces, referenced to both the surface stream function from drifters and to the $27.5\sigma_\theta$ stream function derived from the floats. Results from the two separate reference stream functions are compared in section 5.

3. SPMW Identified as Surface Water Mass

[15] A question to revisit from McCartney and Talley [1982] is whether the winter mixed layer is identical to

SPMW in most of the subpolar gyre. To address this issue we use a larger and more recent hydrographic data set compared with previous studies. Comparing the SPMW depth and the depth of the winter mixed layer, we show that SPMW is always confined within the surface layer and does not subduct below the base of the winter mixed layer.

3.1. SPMW Definition

[16] Subpolar Mode Water is identified here, as previously [e.g., Talley, 1999; Read, 2001], by a minimum of isopycnal potential vorticity (PV), ignoring relative vorticity. The Ertel definition of potential vorticity can be written in terms of the vertical gradient of density,

$$PV = \left| \frac{f}{\rho} \frac{\partial \rho}{\partial z} \right|, \quad (1)$$

where f is the Coriolis parameter and ρ is the density referenced to the midpoint of the depth interval [Talley and McCartney, 1982]. McCartney and Talley [1982] used the Brunt-Vaisala frequency $N^2 = -\frac{g}{\rho} \frac{\partial \rho}{\partial z}$; results are identical in terms of locating the minimum in the vertical density gradient, identified as the SPMW.

[17] The minimum of potential vorticity corresponds to high vertical homogeneity of the water mass and is an appropriate tracer for SPMW. Furthermore, in the absence of mixing, PV is conserved along the flow, hence it is the

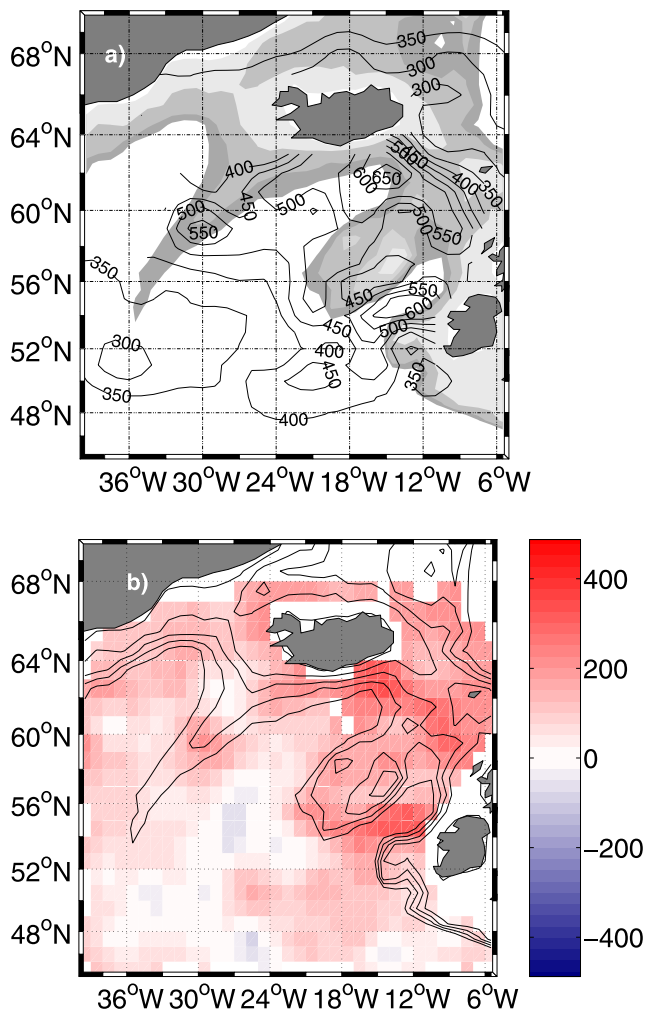


Figure 3. (a) Depth of the winter mixed layer (meters) (see section 3.2). The data have been objectively mapped on a $1^\circ \times 1^\circ$ grid. Topography is shaded, the darkest contour is 2000 m, the lightest is 10 m, and contour interval is 500 m. (b) Difference between the winter mixed layer depth and the SPMW depth (meters). Positive values (red) refer to the base of the winter mixed layer deeper than SPMW, and negative values (blue) refer to the base of the winter mixed layer shallower than SPMW. Contour lines represent the topography. Contour values and interval are as in Figure 3a.

most appropriate dynamical property for tracing water masses horizontally [Talley and McCartney, 1982].

[18] To identify the surface SPMW, we first computed the potential vorticity profile at each station of the historical hydrographic data set and secondly we located the vertical minimum of PV with density lower than $27.7\sigma_\theta$. The density constraint masks the PV minimum associated with the LSW, which, at $27.78\sigma_\theta$, lies below the gyre SPMWs [Talley and McCartney, 1982]. The properties (PV, potential temperature, potential density, depth, salinity) at the minimum of the potential vorticity profile are then bin-averaged on a regular $0.5^\circ \times 0.5^\circ$ grid and objectively mapped (Figure 4 in section 3.3) [Bretherton et al., 1976].

[19] We categorize SPMWs on the basis of potential density. The SPMW potential density varies from approx-

imately $27\sigma_\theta$ to a maximum at the density of Labrador Sea Water, $>27.7\sigma_\theta$ (Figure 4 in section 3.3 and McCartney and Talley [1982]). The northeastern Atlantic is dominated by SPMW in the density range $27.3\sigma_\theta$ to $27.5\sigma_\theta$ (Figure 4b in section 3.3). Therefore we analyze properties on the $27.3\sigma_\theta$, $27.4\sigma_\theta$, and $27.5\sigma_\theta$ isopycnal surfaces; we omit any detailed description of lighter and denser SPMWs, which are located outside our area of interest. On each isopycnal, we identify the SPMW location using low potential vorticity, and then plot its potential temperature, salinity and pressure (Figures 5, 6, and 7 in section 4.1, and section 4.2). The fields obtained using the historical data are smoothed in time and space but provide full regional coverage. The synoptic WOCE cruises provide complementary high resolution but in very limited regions.

[20] Our area of interest (40°W – 0°E , 50°N – 70°N , Figure 2) is confined by the Reykjanes Ridge in the west; Iceland in the north; the Iceland-Faroe Ridge on the north-eastern-eastern edge; and the continental shelf of Great Britain in the east. Figure 2 also shows the historical hydrographic data and WOCE cruise transects.

3.2. Computation of the Winter Mixed Layer Depth

[21] Similarly to McCartney and Talley [1982], profiles at each hydrographic station are used to evaluate the approximate winter mixed layer depth and its properties. Historical temperature profiles are used to estimate the depth of the thermocline marking the base of the winter mixed layer.

[22] The winter stations clearly show a thermocline deeper than 200 m associated with the base of the winter mixed layer [McCartney and Talley, 1982]. Late spring and summer stations have a near-surface thermocline associated with the summer stratification. Stations collected in the warm months are also characterized by another deeper thermocline, identified as the base of the remnant winter mixed layer [McCartney and Talley, 1982]. To approximate the winter mixed layer depth, we identify the largest vertical temperature gradient between 200 and 1000 m for each temperature profile (from all months). This depth range excludes the shallow summer stratification and reduces the possible bias due to poor sampling for depths larger than 1000 m. The depths from all profiles are then bin averaged and objectively mapped on a uniform $1^\circ \times 1^\circ$ grid [Bretherton et al., 1976].

[23] The gradient method used in the present paper overestimates the winter mixed layer depth. A curvature method, in which the remnant winter mixed layer depth is associated with a maximum curvature (second derivative of temperature), can provide a more accurate estimate of the depth for many profiles. However, many complex or undersampled profiles have to be excluded, which degrades the overall estimate of mixed layer depth using this method (not shown). Nonetheless, the curvature method can be used to estimate the bias in the gradient method for those profiles that have “good” second derivatives, defined as being within 150 m of the maximum gradient. Of 7223 profiles overall used in estimating winter mixed layer depth using the gradient method, 6613 profiles also had good second derivatives; the depth of the maximum gradient was 40 m deeper than the depth of the maximum curvature for the many profiles with good second derivatives, which is thus

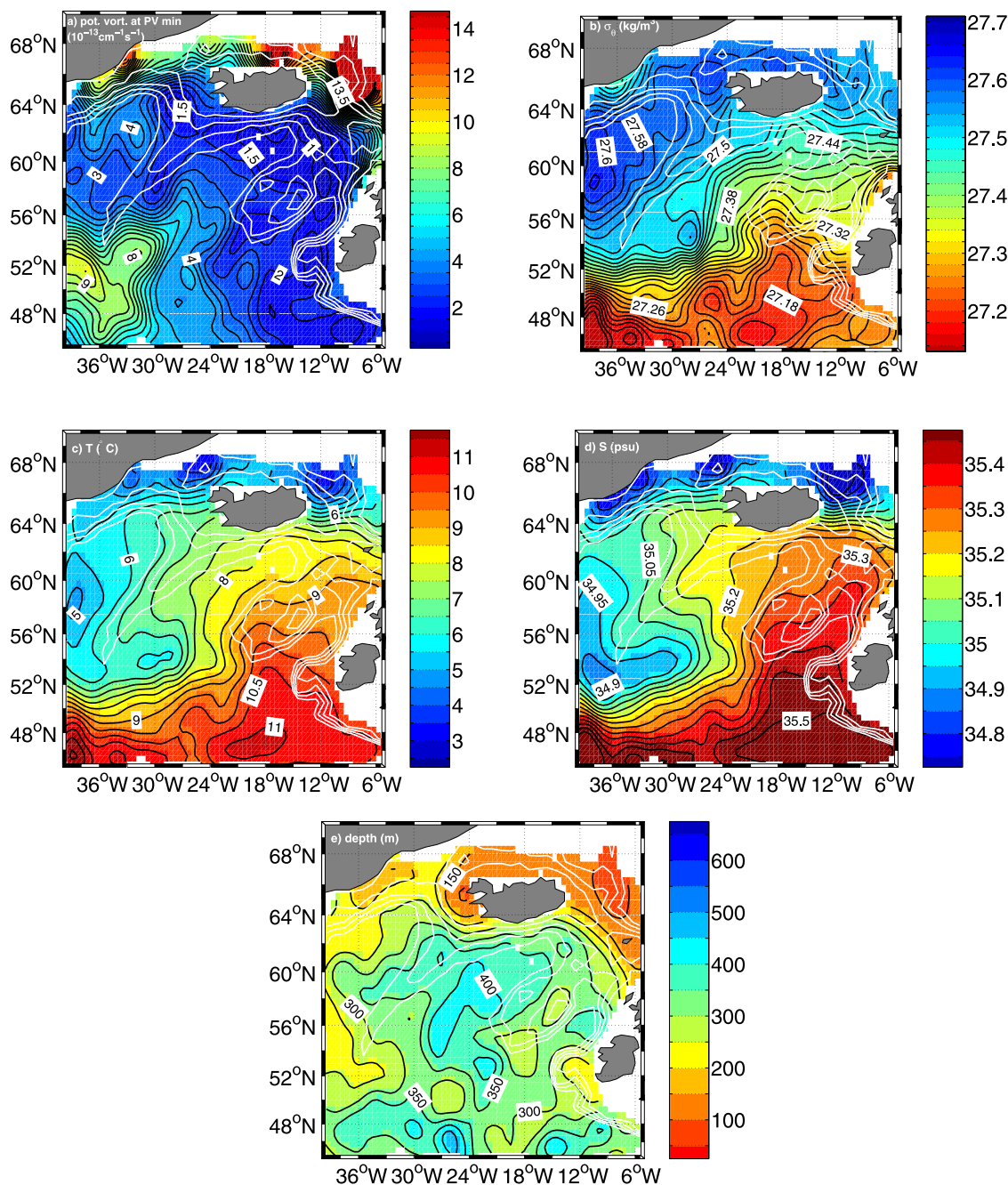


Figure 4. Properties at the PV minimum with density lower than $27.7\sigma_\theta$. The property maps are obtained by bin-averaging the historical hydrographic measurements and objectively mapping the mean field on a uniform $0.5^\circ \times 0.5^\circ$ grid. White contours are the topography from 2000 m to 10 m; the contour interval is 500 m. (a) Potential vorticity $10^{-13} \text{ cm}^{-1} \text{ s}^{-1}$. (b) Potential density ($\sigma_\theta - 1000$), contour interval 0.02 kg/m^3 . (c) Potential temperature ($^\circ\text{C}$), contour interval 0.5°C . (d) Salinity (psu), contour interval 0.05 psu . (e) Depth (meters), contour interval 50 m.

our estimate of the bias of the mixed layer depth using the gradient method.

3.3. Argument Against Subduction of SPMW

[24] Vertical convection during winter leads to the formation of a deep, well-mixed surface layer in the subpolar North Atlantic (Figure 3). Consequently, this process has been considered the major origin of SPMW [McCartney and Talley, 1982]. Thus we first present the winter mixed

layer to compare with the SPMW (see section 3.2), which is identified by regions of low PV. This permits us to investigate whether SPMW is subducted anywhere in this domain. (On the basis of the prevalence of positive wind-stress curl in this region, we do not expect to find classical subduction. Nevertheless, it is important to evaluate this possibility, especially in light of the formation calculation in the companion paper [Brambilla et al., 2008].)

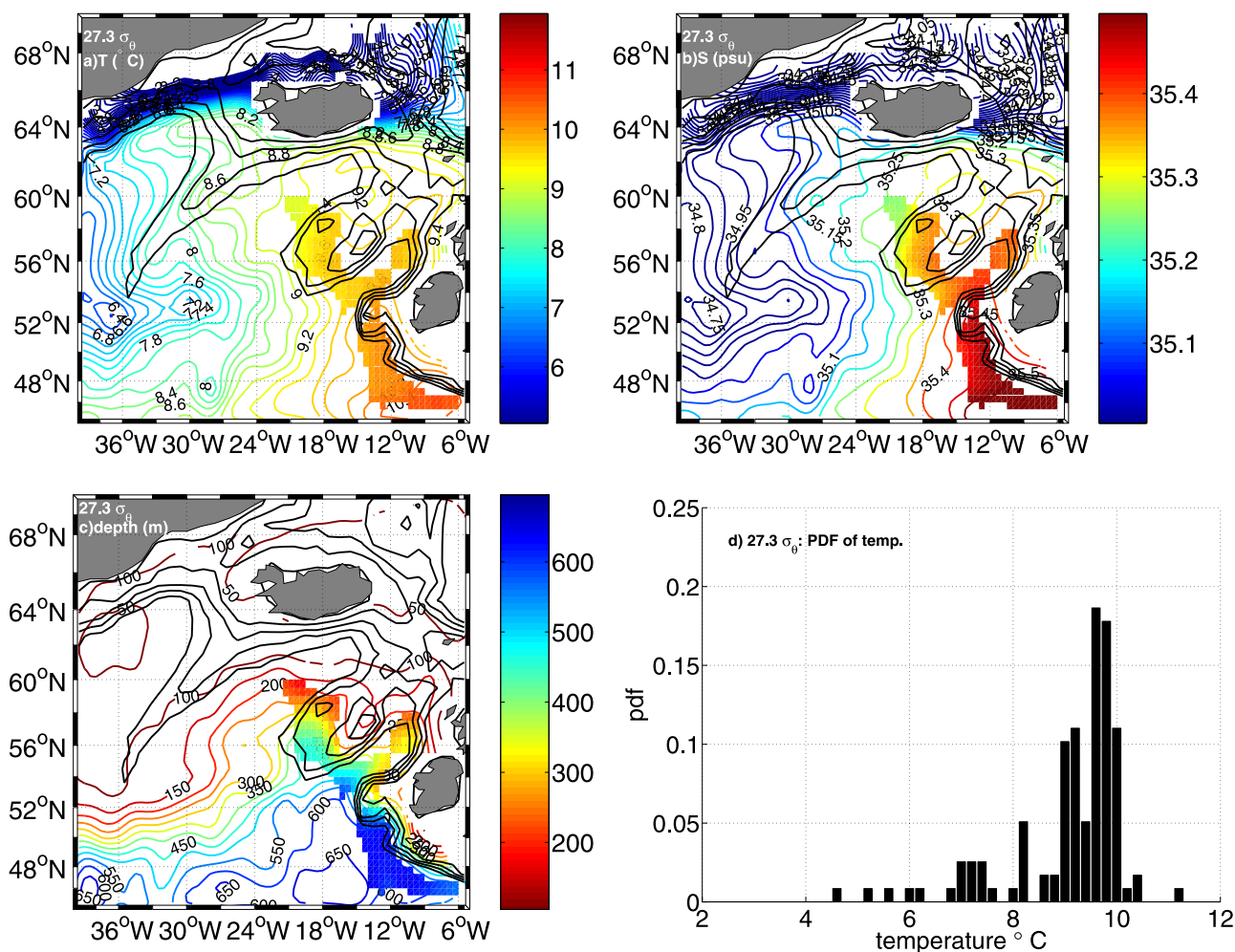


Figure 5. Properties at $27.3\sigma_\theta$. Colored contours are the values on the entire isopycnal surface; the filled colors are the property values limited to the areas where the potential vorticity is less than $10 \times 10^{-13} \text{ cm}^{-1} \text{ s}^{-1}$. Black contours represent the topography. The deepest contour is at 2000 m, the shallowest is at 10 m, and the contour interval is 500 m. (a) Potential temperature ($^\circ\text{C}$), contour interval 0.2°C ; (b) salinity (psu), contour interval 0.05 psu; (c) depth (meters), contour interval 50 m. (d) Probability density function (pdf) of temperature from historical hydrographic stations with low values of potential vorticity (stations present in the filled color area). The limited number of data might bias the pdf.

[25] The greatest winter mixed layer depths (Figure 3) are in Rockall Trough (~ 600 m) and on the northeastern edge of the Iceland Basin, where the winter mixed layer reaches ~ 650 m. The depth decreases toward the topographic features. On the eastern flank of the Reykjanes Ridge it is 450–500 m; on the Iceland-Faroe Ridge it is ~ 400 m. The base of the mixed layer in the center of the Iceland basin is ~ 500 m. (Depths are not mapped in the Irminger Sea because of large error due to the difficulty in locating the winter thermocline in the temperature profiles of this region.) These values are consistent with the older mixed layer depth estimates from *McCartney and Talley* [1982] and *Qiu and Huang* [1995], and with the recent estimates from *Kara et al.* [2003] and *de Boyer Montégut et al.* [2004].

[26] We then compare the depth of the winter thermocline to the depth of the SPMW. The latter has been evaluated at each hydrographic station by looking at the depth of the minimum of potential vorticity in the water column, excluding densities larger than $27.7\sigma_\theta$ (Figure 4e), following

the definition of section 3.1. For a simple mixed layer that is identical with SPMW, the PV minimum will always be shallower than the thermocline depth used to estimate the base of the winter mixed layer.

[27] The difference between the base of the winter mixed layer and the SPMW pycnostad depth is shown in Figure 3b. For positive values (red) the base of the winter mixed layer is greater than the SPMW PV minimum. The values are predominantly positive throughout the eastern subpolar gyre. The SPMW PV minimum is, on average, ~ 100 m shallower than the base of the winter mixed layer (which is effectively a PV maximum). Thus it can be concluded that the winter mixed layer is representative of the SPMW, within the standard deviation [$O(100$ m)] associated with the mean values of the depth of the remnant of the winter mixed layer. This result agrees with *McCartney and Talley's* [1982] conclusion. On the isopycnals considered, there is no indication of subduction of the SPMW PV minimum below the base of the winter mixed layer. Lower density SPMWs,

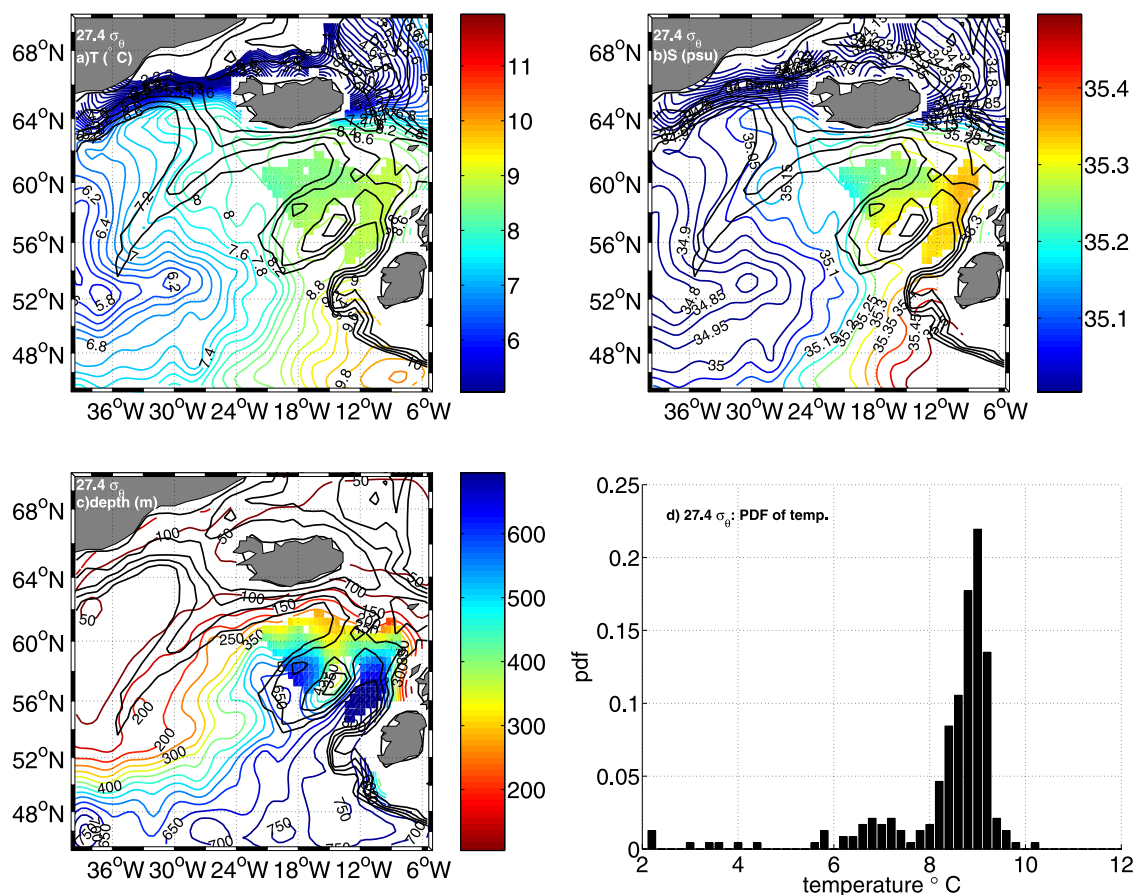


Figure 6. Properties at $27.4\sigma_\theta$. Colored contours are the values on the entire isopycnal surface; the filled colors are the property values limited to the areas where the potential vorticity is less than $8 \times 10^{-13} \text{ cm}^{-1} \text{ s}^{-1}$. Black contours represent the topography. The deepest contour is at 2000 m, the shallowest is at 10 m, and the contour interval is 500 m. (a) Potential temperature ($^{\circ}\text{C}$), contour interval 0.02°C ; (b) salinity (psu), contour interval 0.05 psu; (c) depth (meters), contour interval 50 m. (d) The pdf of temperature from historical hydrographic stations with low values of potential vorticity (stations present in the filled color area). The limited number of data might bias the pdf.

not considered here, do subduct to the south [McCartney, 1982; Harvey and Arhan, 1988]. (The negative values in the southern Iceland basin and south of 52°N , of the order of 25 m, are within the uncertainty of the computation.)

[28] This confirmation of the lack of visible subduction of SPMW is important because the air-sea flux calculation presented in the companion paper [Brambilla et al., 2008] shows large regions of “formation” (water mass convergence). In water mass transformation and formation calculations based on air-sea fluxes [e.g., Speer and Tziperman, 1992; Marshall et al., 1999], water mass formation is usually interpreted as subduction, in which properties of the mixed layer, including its PV, are advected smoothly down along isopycnals. Since the PV minimum is shallower than the base of the winter thermocline, SPMWs in the northeastern North Atlantic do not subduct, unlike Subtropical Mode Water [Worthington, 1976; Hanawa and Talley, 2001] and unlike the lightest forms of SPMW [McCartney, 1982]. Therefore the net formation of SPMW, obtained in the subsequent paper, is interpreted as loss by entrainment to the interior layers (e.g., at the Nordic Seas overflows and

into Labrador Sea Water), with associated vigorous mixing that severely alters the surface layer (SPMW) properties.

4. SPMW Distribution

[29] The original description of SPMW by McCartney and Talley [1982] emphasizes the cyclonic arrangement of SPMWs of increasing density around the subpolar gyre with the implication of a continuous cyclonic flow connecting them sequentially. More recent studies [Talley, 1999; Read, 2001] suggest that patches of SPMW are horizontally separated by stratified water masses. Here, moving toward the resolution of this disagreement, we further investigate the SPMW distribution and properties. We then interpret SPMW in terms of the stream function (section 5).

4.1. SPMW Properties

[30] As described in section 3.1, SPMWs are identified by especially low potential vorticity values at the PV minimum. (A single PV cutoff value for mode water identification is often applied [Hanawa and Talley, 2001], but a specific

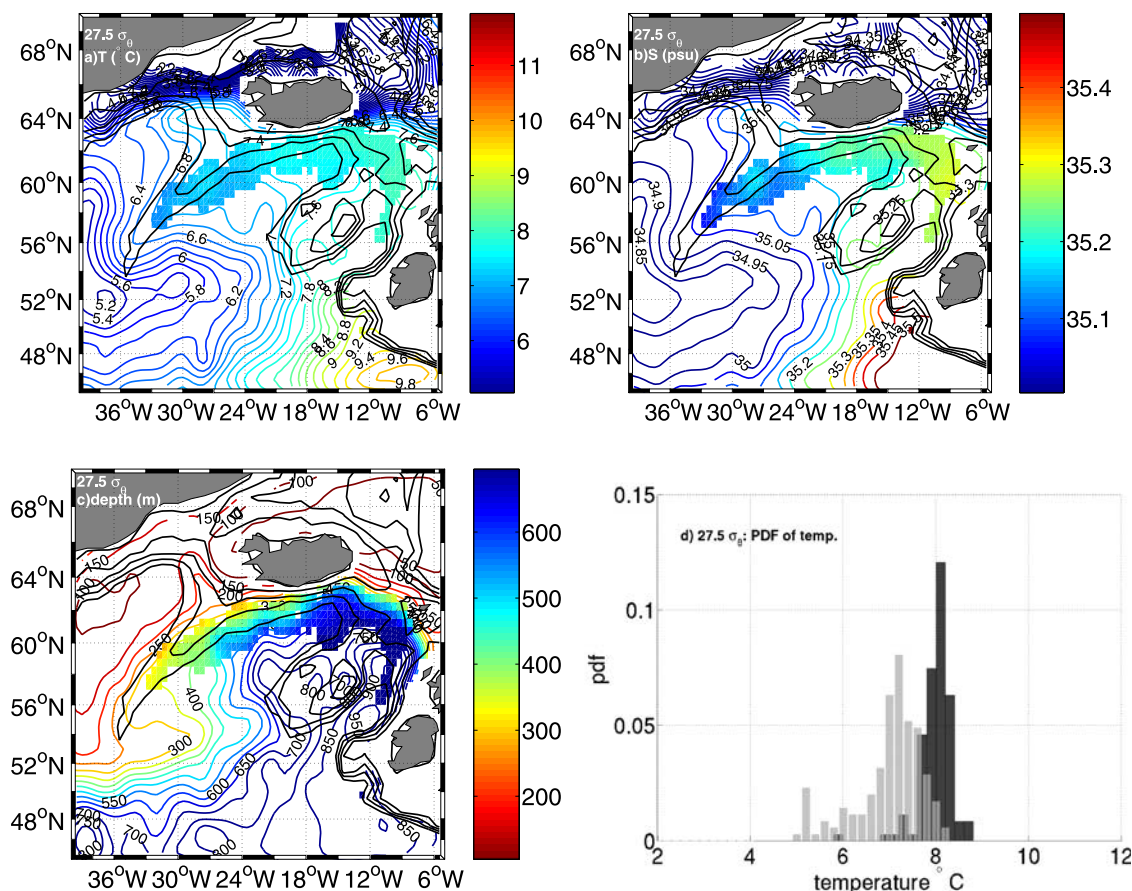


Figure 7. Properties at $27.5\sigma_\theta$. Colored contours are the property values on the entire isopycnal surface; the filled colors are the property values limited to the areas where the potential vorticity is less than $8 \times 10^{-13} \text{ cm}^{-1} \text{ s}^{-1}$. Black contours represent the topography. The deepest contour is at 2000 m, the shallowest is at 10 m, and the contour interval is 500 m. (a) Potential temperature ($^\circ\text{C}$), contour interval 0.02°C ; (b) salinity (psu), contour interval 0.05 psu; (c) depth (meters), contour interval 50 m. (d) The pdf of temperature from historical hydrographic stations with low values of potential vorticity (stations present in the filled color area). The limited number of data might bias the pdf. In gray is the temperature pdf of the $27.5\sigma_\theta$ SPMW on the Reykjanes Ridge, and in black is the temperature of the $27.5\sigma_\theta$ SPMW on the Iceland-Faroe Ridge.

choice would be unnecessarily arbitrary here. Depending on the application, i.e., isopycnal surfaces, different cutoff values are used. These are shown in Figures 5, 6, and 7, and Figure 10 in section 4.3.) The lowest values of potential vorticity are detected southwest of Porcupine Bank, on the southern Rockall Plateau, and over the northwestern Reykjanes Ridge. In contrast, large mean values of potential vorticity at the PV minimum are associated with the strongest currents of the region: the NAC that flows eastward into the study domain, the northern side of the Iceland-Faroe Front, and the East Greenland Current, none of which are characterized by SPMW [McCartney and Talley, 1982; Harvey and Arhan, 1988; Talley, 1999].

[31] In the Iceland Basin, Talley [1999], using synoptic data, showed that the NAC (Subarctic front) is characterized by large potential vorticity and therefore by the absence of SPMW. This high potential vorticity region is not present in Figure 4a. Instead, the mean potential vorticity is quite low in the entire Iceland Basin. The difference is likely due to our use of an average field that smooths out the NAC front,

whose location and intensity vary in time and space [Flatau *et al.*, 2003].

[32] In the Irminger Sea, we expected to find very low potential vorticity associated with the SPMW precursor of LSW [Talley, 1999; Pickart *et al.*, 2003]. The high PV found there is most likely due to the density cutoff we used to separate SPMW and LSW. Since the density of the SPMW in the Irminger Sea is very close to $27.7\sigma_\theta$, such a cutoff does not allow a proper mapping of the actual potential vorticity values. The unrealistically shallow depth of the PV minimum in the Irminger Sea also confirms this.

[33] The density of the PV minimum in the eastern subpolar gyre, starting approximately from $27.3\sigma_\theta$, increases smoothly following two main directions: northeastward, in the Rockall Trough and Iceland Basin, and westward, from the Reykjanes Ridge to the Irminger Sea. In the Rockall Trough, the potential density varies from $27.28\sigma_\theta$ to $27.38\sigma_\theta$; in the Iceland Basin, from $27.38\sigma_\theta$ to $27.48\sigma_\theta$; on the Reykjanes Ridge, from $27.42\sigma_\theta$ to $27.56\sigma_\theta$. (SPMW properties are patchy when mapped synoptically but still appear to increase downstream [Talley, 1999; Read, 2001].)

Table 1. Mean and Standard Deviation of Potential Temperature, Salinity, and Depth for Each SPMW

	Θ , °C	S, psu	D, m
27.3 σ_θ	9.82 \pm 0.37	35.41 \pm 0.083	453 \pm 145
27.4 σ_θ	8.64 \pm 0.20	35.29 \pm 0.04	481 \pm 143
27.5 σ_θ - Iceland-Faroe Ridge	7.81 \pm 0.21	35.25 \pm 0.04	670 \pm 143
27.5 σ_θ - Reykjanes Ridge	7.28 \pm 0.24	35.15 \pm 0.04	435 \pm 86

The connection between the mean properties of the SPMWs and the subpolar gyre circulation is fully explored in section 5.

4.2. SPMW on Isopycnal Surfaces

[34] A different way to illustrate the properties of SPMW, more convenient to investigate its connecting pathways, is to look at isopycnals that intersect the SPMW (colored background of Figure 10 in section 4.3). Here we identify SPMWs by low potential vorticity along the desired isopycnal, and describe the associated potential temperature, salinity and depth in the low potential vorticity region (Figures 5, 6, and 7). We show results for the 27.3 σ_θ , 27.4 σ_θ , and 27.5 σ_θ isopycnals.

[35] At 27.3 σ_θ , there are three main regions of low PV: west of Porcupine Bank, in the southern Rockall Trough, and on the southwestern flank of Rockall Plateau. The 27.4 σ_θ SPMW is located on both the western flank of Rockall Plateau and in the northern part of Rockall Trough. The 27.5 σ_θ SPMW is located on both the Iceland-Faroe Ridge and on the eastern and southern flank of the Reykjanes Ridge.

[36] The location of the 27.3 σ_θ and 27.4 σ_θ SPMW agrees with the isopycnal potential vorticity maps shown by Talley [1999], based on a sparser historical data set. The location of the 27.5 σ_θ SPMW exhibits some differences due to the much larger hydrographic data set used here. In work by Talley [1999], the 27.5 σ_θ SPMW is shown only on the Reykjanes Ridge, while here we identify 27.5 σ_θ SPMW on both the Reykjanes and the Iceland-Faroe Ridges.

[37] The comparison of the PV fields on these three isopycnals, shows that the low PV visually proceeds northeastward with increasing potential density, in both the Iceland Basin and the Rockall Trough, while it veers westward-southwestward along the Reykjanes Ridge passing from 27.4 σ_θ to 27.5 σ_θ . As discussed in section 5, the gradual densification of the low PV regions in each basin is due to the link between the subpolar gyre circulation, which is strongly influenced by the topography, and the SPMW.

[38] Potential temperature, salinity, and depth of the SPMW on each isopycnal (27.3 σ_θ , 27.4 σ_θ , 27.5 σ_θ) are shown in Figures 5, 6, and 7 with mean values listed in Table 1. The filled colors are the values limited to regions of potential vorticity lower than $10 \times 10^{-13} \text{ cm}^{-1} \text{ s}^{-1}$ at 27.3 σ_θ , and lower than $8 \times 10^{-13} \text{ cm}^{-1} \text{ s}^{-1}$ at 27.4 σ_θ and 27.5 σ_θ , while the contours represent the property values elsewhere. The property fields obtained here from historical hydrographic data are in good agreement with those obtained in the same region from the quasi-synoptic hydrographic data set collected during the Vivaldi cruise [Pollard *et al.*, 2004]. However, it is noteworthy that the salinity at 27.4 σ_θ from the quasi-synoptic data set is ~ 0.1 psu fresher than that obtained from historical data.

[39] Figures 5, 6, and 7 confirm a smooth progression of SPMW properties northeastward through the Iceland Basin

and Rockall Trough, and westward-southwestward along the Reykjanes Ridge. The decrease of hydrographic properties is likely associated with heat loss in the subpolar gyre that drives the temperature decrease and shoaling of the isopycnals [Brambilla *et al.*, 2008].

[40] In addition to the regional distribution of the properties of the 27.3 σ_θ , 27.4 σ_θ , and 27.5 σ_θ SPMW, we also show the temperature probability distribution (Figures 5d, 6d, and 7d) to better describe the lateral homogeneity of the SPMWs. The probability distribution of temperature is computed from the hydrographic stations characterized by low PV (stations in the filled color areas in Figures 5a, 6a, and 7a), without averaging the data. The 27.3 σ_θ and 27.4 σ_θ SPMW are characterized by a nearly Gaussian distribution suggesting that these SPMWs are laterally nearly homogeneous around a mean value. (In both 27.3 σ_θ and 27.4 σ_θ SPMW, the tail toward colder temperature is due to a few stations in the southern Iceland Basin.) In contrast, the temperature probability distribution of the 27.5 σ_θ SPMW is bimodal (Figure 7d), indicating two separate types of the same density SPMW, occupying different regions: the Reykjanes Ridge and the Iceland-Faroe Ridge. The 27.5 σ_θ SPMW on the Reykjanes Ridge is colder and fresher compared with the 27.5 σ_θ SPMW on the Iceland-Faroe Ridge. This suggests that the sources of these two SPMWs with the same density differ, possibly associated with separate currents (see section 5.1).

4.3. Seasonal Variation of SPMW Location

[41] Seasonal variability of SPMW has not been examined previously. SPMW properties are set in the winter, while the circulation that advects the SPMW continues through all seasons. Thus SPMW for a given winter should move downstream and thus yield a seasonal cycle of SPMW at each location. To examine this possibility for the 27.3 σ_θ –27.5 σ_θ SPMWs, there is enough historical hydrographic data in the northeastern Atlantic (east of the Reykjanes Ridge, north of 52°N) in spring (AMJ), summer (JAS), and fall (OND) (Figure 8). Winter (JFM) coverage in this region is not adequate. (Although there are numerically more winter than autumn data, winter data are concentrated in specific locations and do not provide enough spatial coverage.) SPMW seasonal evolution is illustrated with the seasonal shift of the blue dots (PV lower than $4 \times 10^{-13} \text{ cm}^{-1} \text{ s}^{-1}$ indicating the presence of SPMW, Figure 9). The underlying mean potential vorticity field for the whole region during the three seasons on the three isopycnals 27.3 σ_θ , 27.4 σ_θ , 27.5 σ_θ is computed from the entire seasonal data set (including the data south of 52°N and west of the Reykjanes Ridge) and objectively mapped on a regular $0.5^\circ \times 0.5^\circ$ grid (Figure 9).

[42] At 27.3 σ_θ and 27.4 σ_θ , the location of the lowest potential vorticity (i.e., the location of the most extreme SPMW) appears to proceed northeastward with advancing seasons along the Iceland Basin and the Rockall Trough. The seasonal displacement is in agreement with the direction of the mean flow of the region (Figure 10), suggesting advection of these SPMWs following formation in late winter. At 27.5 σ_θ , the bin-average potential vorticity field does not show an annual progression, probably because of poor spatial distribution of the seasonal data. However, an annual advection is presented by the hydro-

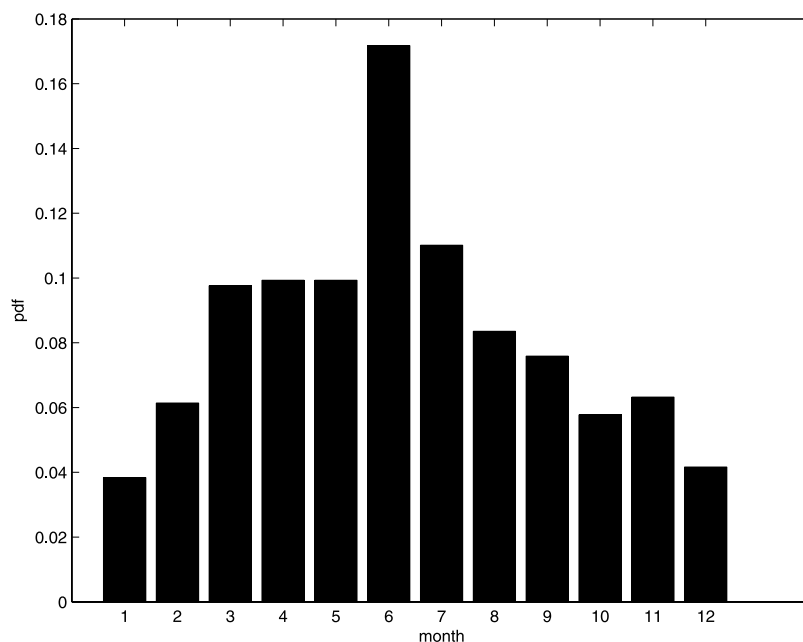


Figure 8. Monthly distribution of the entire hydrographic data. The winter data (JFM) are mostly located in the Irminger Sea and south of 52°N ; thus they are not adequate to analyze the $27.3\sigma_{\theta}$ – $27.5\sigma_{\theta}$ SPMWs.

graphic stations identifying the $27.5\sigma_{\theta}$ SPMW. The subgroup of stations characterized by low PV at $27.5\sigma_{\theta}$ proceeds northeastward along the Irminger Current from spring to summer.

5. Circulation in the Eastern Subpolar Gyre

[43] Mode waters are generally associated closely with the warm side of major currents [e.g., *McCartney and Talley*, 1982; *Harvey and Arhan*, 1988; *Hanawa and Talley*, 2001]. New understanding of the strength of the several branches of the NAC in the northeastern Atlantic [*Arhan*, 1990; *Orvik and Niiler*, 2002; *Niiler et al.*, 2003; *Flatau et al.*, 2003] suggests that we reexamine the relation of SPMW to the circulation in the region. The downstream SPMW evolution coincides with the directions of the branches of the NAC in Rockall Trough and the Iceland Basin (section 4.2). Here we show the visual correspondence between the surface stream function and the direction in which the SPMW density increases. Then, to better quantify the association between the averaged SPMW and the mean NAC branches, we compute the joint probability density function between the potential vorticity on each isopycnal and the estimated values of the surface stream function.

5.1. Surface Circulation

[44] The surface stream function computed from surface drifters drogued at 15 m (black contours in Figure 10, computation described in Appendix A) reproduces previous results [*Fratantoni*, 2001; *Orvik and Niiler*, 2002; *Reverdin et al.*, 2003; *Niiler et al.*, 2003; *Flatau et al.*, 2003]. From the northwestern corner at $\sim 50^{\circ}\text{N}$, 50°W [*Rosby*, 1996], the NAC flows eastward between 47°N and 52°N , crossing the North Atlantic basin. As suggested also by hydrographic studies [e.g., *Bubnov*, 1968; *Harvey and Arhan*, 1988; *Arhan*, 1990], the eastward NAC system

consists of two parallel branches that cross the Mid-Atlantic Ridge (MAR) at different latitudes. The southern branch crosses the MAR at 47°N – 48°N , the northern branch at 51°N – 52°N . Furthermore, *Sy* [1988] proposed that an additional third branch exists and meanders between the other two. The northern and the southern branches of the NAC are the predecessors of the northeastward Iceland Basin and the Rockall Trough branches of the NAC, respectively, that are clearly tracked by the surface stream function.

[45] The Iceland Basin branch of the NAC likely consists of two distinguishable currents (Figure 10), as shown by *Niiler et al.* [2003], using the same drifter data set. One current is located along the western flank of the Rockall Plateau (Subarctic Front), and the other in center of the Iceland Basin between 28°W and 24°W (Central Iceland Basin branch of the NAC). The currents are parallel up to 61°N , where part of the latter veers westward and joins the East Reykjanes Ridge Current along the eastern flank of the Reykjanes Ridge [*Orvik and Niiler*, 2002]. In the work by *Niiler et al.* [2003], a similar double structure of the northeastward flow of the Iceland Basin is suggested by the presence of two fast branches in the Iceland Basin.

[46] Geostrophic velocity from the WOCE A24 cruise, Greenland-Scotland transect (not shown), confirms the double structure. Similarly, *Pollard et al.*'s [2004] Vivaldi 1996 cruise showed the Central Iceland Basin and the Subarctic Front branches of the NAC in the Iceland Basin.

[47] To track the location of SPMW along the complex system of currents of the Iceland Basin and Rockall Trough, we superimpose the surface stream function on the potential vorticity field at $27.3\sigma_{\theta}$, $27.4\sigma_{\theta}$ and $27.5\sigma_{\theta}$ (Figure 10). Similarly to section 4.1, low values of potential vorticity are used to identify SPMW.

[48] Visual interpretation of the following plots (Figure 10) suggests that SPMW is advected along the mean path of each subpolar gyre current. However, caution

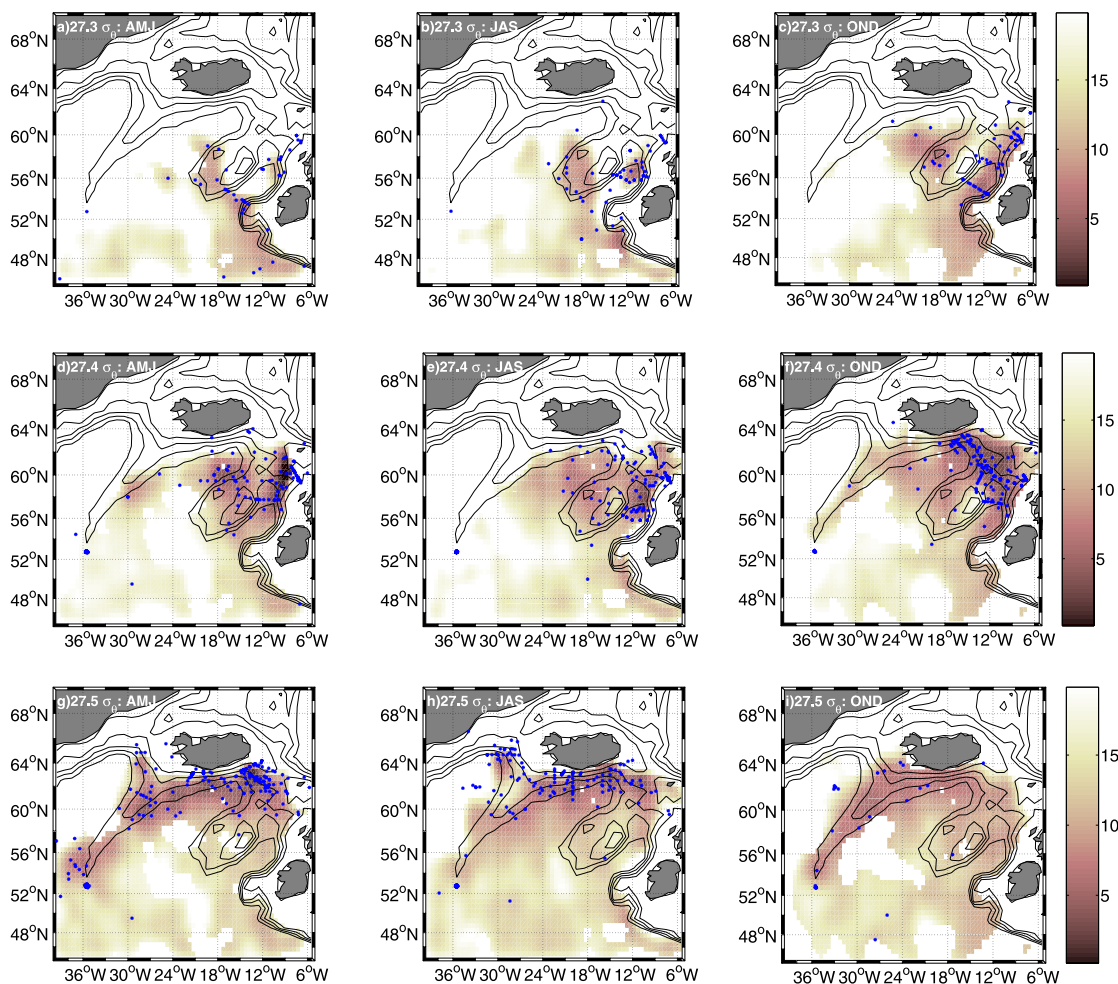


Figure 9. Seasonal potential vorticity ($10^{-13} \text{ cm}^{-1} \text{ s}^{-1}$) objectively mapped on a uniform $0.5^\circ \times 0.5^\circ$ grid. Black contours represent the topography. The deepest contour is at 2000 m, the shallowest is at 10 m, and contour interval is 500 m. On each plot the blue asterisks refer to the hydrographic stations with PV less than $4 \times 10^{-13} \text{ cm}^{-1} \text{ s}^{-1}$, on the corresponding isopycnal and during the corresponding season: (a) $27.3\sigma_\theta$, spring; (b) $27.3\sigma_\theta$, summer; (c) $27.3\sigma_\theta$, fall; (d) $27.4\sigma_\theta$, spring; (e) $27.4\sigma_\theta$, summer; (f) $27.4\sigma_\theta$, fall; (g) $27.5\sigma_\theta$, spring; (h) $27.5\sigma_\theta$, summer; and (i) $27.5\sigma_\theta$, fall.

is advised. Because of the temporal and spatial averaging of the hydrographic data used to identify SPMW and for the stream functions, the precise relationship between the location of a given SPMW and a current core is smeared out. The synoptic association of SPMW with a given strong current is advection along the warm side of the current, not at the core of the current [Talley, 1999; McCartney and Talley, 1982; Hanawa and Talley, 2001]. Thus, hereafter, consistent with Figure 10, when we refer to SPMWs as advected along the mean flow, we mean advection along the warm side of the current. Even though the smoothed fields do not permit the SPMW to be precisely located relative to the narrow synoptic current cores, the superposition of surface stream function and potential vorticity fields allows to clearly associate SPMWs of different densities with the various subpolar gyre currents.

[49] The $27.3\sigma_\theta$ SPMW in Rockall Trough is located along the Rockall Trough branch of the NAC. The $27.3\sigma_\theta$ SPMW located along the western flank of the Rockall Plateau is present along both the Subarctic Front and the

Central Iceland Basin branch of the NAC (Figure 10a). The lowest PV values appear to be associated with the Subarctic Front. The minimum of PV at the western edge of the British continental shelf is marginally associated with the southern part of the Rockall Trough branch of the NAC. However here the error in the computation of the surface stream function is quite large (50%) and therefore might bias the direction of the streamlines.

[50] The $27.4\sigma_\theta$ SPMW (Figure 10b) is also located along the Rockall Trough branch of the NAC, and the Subarctic Front and Central Iceland Basin branch of the NAC. The position of the $27.4\sigma_\theta$ SPMW is slightly downstream of the lighter $27.3\sigma_\theta$ SPMW, suggesting that the former is derived from the latter.

[51] The densest SPMW considered ($27.5\sigma_\theta$) (Figure 10c) is associated with both the southern side of the Iceland-Faroe Front and the East Reykjanes Ridge Current. The $27.5\sigma_\theta$ SPMW along the southern side of the Iceland-Faroe Ridge is likely derived from two separate sources. The $27.5\sigma_\theta$ SPMW located at the southeastern end of the

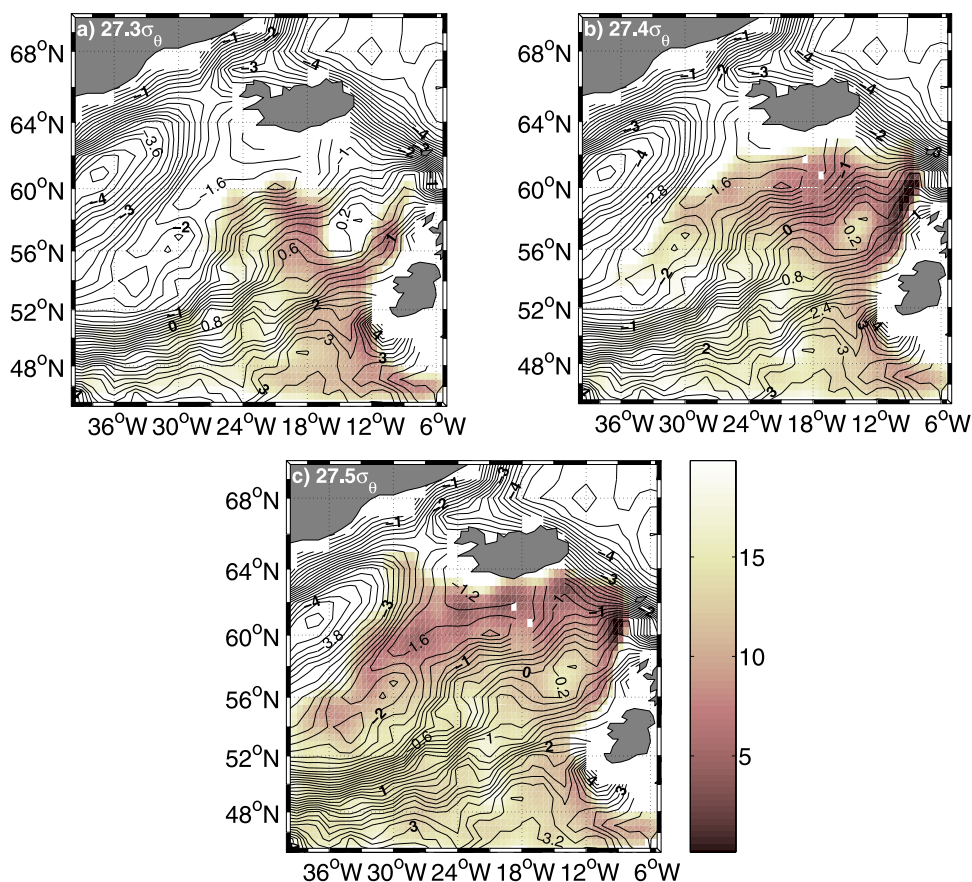


Figure 10. Absolute surface stream function ($\text{m}^2 \text{s}^{-2}$, contours interval $0.2 \text{ m}^2 \text{s}^{-2}$) based on surface drifters with Ekman removed, superimposed on the potential vorticity field ($10^{-13} \text{ cm}^{-1} \text{ s}^{-1}$): (a) $27.3\sigma_\theta$; (b) $27.4\sigma_\theta$; and (c) $27.5\sigma_\theta$. A schematic that summarizes the currents shown by the surface stream function is presented in Figure 1.

Iceland-Faroe Ridge (closest to Scotland) might originate from the $27.4\sigma_\theta$ SPMW advected along the Rockall Trough Branch of the NAC. The $27.5\sigma_\theta$ SPMW located toward the central and northwestern end of the Iceland-Faroe Ridge is probably derived from the $27.4\sigma_\theta$ SPMW along the Subarctic Front, which flows along the western flank of Rockall Plateau. The $27.5\sigma_\theta$ SPMW located along the East Reykjanes Ridge Current might be connected, instead, to the lower density SPMW along the Central Iceland Basin branch of the NAC part of which becomes the East Reykjanes Ridge Current.

[52] SPMWs east of the Subarctic Front are very unlikely to be the source of SPMWs on the Reykjanes Ridge west of the front. This is apparent from the different potential temperature-salinity characteristics of the two regions. On the synoptic WOCE A24 cruise (Figure 11), the Subarctic Front (blue stations) separates the fresher Subarctic Intermediate Water (SAIW) to the west from the saltier North Atlantic Water (NAW) to the east [Harvey and Arhan, 1988; Talley, 1999; Pollard *et al.*, 2004]. Waters in the eastern Iceland Basin, the Subarctic Front, and the Rockall Trough branch of the NAC (black, blue, red, yellow stations) are warmer and saltier than the water carried by the western side of the Central Iceland Basin branch of the NAC (magenta stations), especially at densities lower than $27.4\sigma_\theta$. Thus we hypothesize that the warmer and saltier flow feeds the

warmer and saltier Iceland-Faroe SPMW, while the fresher and cooler flow (western side of the Central Iceland Basin branch of the NAC) feeds the fresher and cooler Reykjanes Ridge SPMW (Figure 7). Moreover, the western side of the Central Iceland Basin branch of the NAC has properties similar to those on the Reykjanes Ridge (Figure 7), confirming that this current most likely provides water to the Reykjanes Ridge.

[53] The joint probability density function (pdf) computed along each isopycnal ($27.3\sigma_\theta$, $27.4\sigma_\theta$, $27.5\sigma_\theta$, Figure 12) between the PV and the surface stream function values, interpolated at the location of the hydrographic stations, confirms the visual link between SPMW and NAC branches (Figure 10). The largest values of the joint pdf for low values of PV correspond to the stream function values that characterize the surface currents along which SPMWs have been visually tracked. (In Figure 12c, the high pdf values at $-2 \text{ m}^2/\text{s}^2$ are due to an extremely dense concentration of hydrographic stations at the southern tip of the Reykjanes Ridge (Figure 2)).

[54] Thus, in contrast to the description of McCartney and Talley [1982], who hypothesized that all SPMWs are connected by a continuous cyclonic flow, we have shown that the cyclonic SPMW path is limited to a weak circulation that joins the western side of the Central Iceland Basin branch of the NAC to the east Reykjanes Ridge Current.

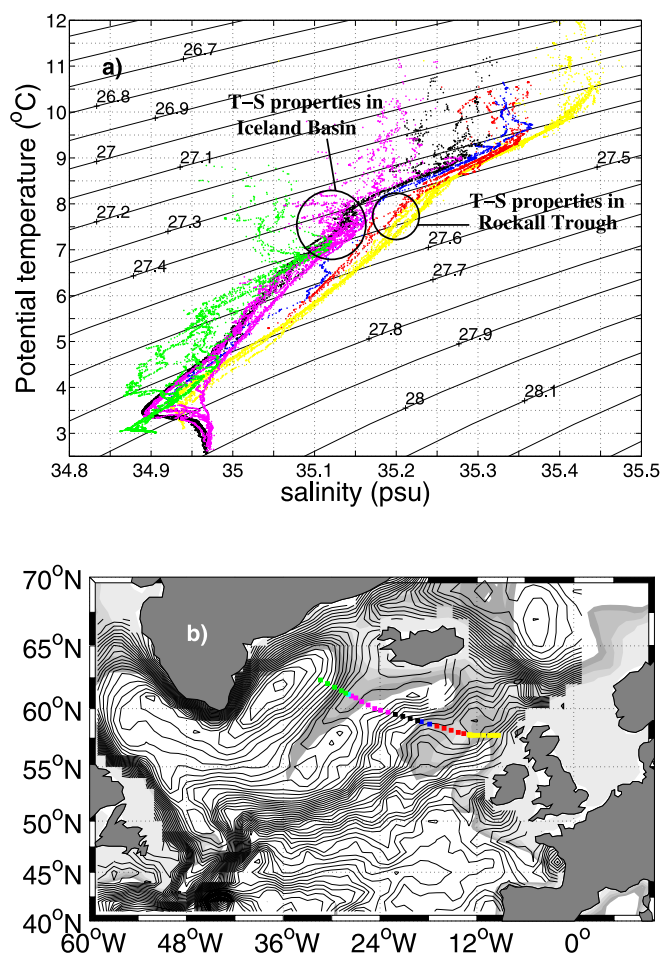


Figure 11. (a) Potential temperature-salinity curves from hydrographic data of the A24 WOCE cruise, Greenland-Scotland transect. The different colors refer to the color coded stations along the transect. The stations in the Irminger Sea have not been plotted. (b) Greenland-Scotland transect for the A24 cruise. Stations in the Irminger Sea have not been plotted. The colors correspond to the profiles plotted in Figure 11a. The black contours represent the surface stream function plotted in Figure 10.

The dominant surface flow, instead, is characterized by a strong northeastward flows that transport SPMW to the Norwegian Current (Subarctic Front, Rockall Trough branch of the NAC, and, partially, Central Iceland Basin branch of the NAC). The warm side of each of the NAC branches in the eastern subpolar gyre is characterized by progression of SPMWs with gradually increasing density (from $27.3\sigma_\theta$ to $27.5\sigma_\theta$, as shown earlier in Figure 1). Thus a smooth downstream progression of SPMW properties, which was an element of *McCartney and Talley's* [1982] description, is valid for each separate current. However, a broad connection of, say, the $27.3\sigma_\theta$ SPMW in the Rockall Trough with the $27.5\sigma_\theta$ SPMW of the Reykjanes Ridge (and hence the Irminger Sea) is highly unlikely.

5.2. Stream Functions on Isopycnal Surfaces

[55] The surface absolute stream function (section 5.1) shows that the surface flow is predominantly northeastward, with a weak cyclonic circulation that connects the western side of the Central Iceland Basin branch of the NAC to the East Reykjanes Ridge Current. It could be argued that the westward diapycnal flow that departs from the Central

Iceland Basin branch is not sufficient to provide the water mass that is part of the extended $27.5\sigma_\theta$ SPMW located on the Reykjanes Ridge (Figure 10). Thus we provide a qualitative description of the subsurface circulation on the $27.3\sigma_\theta$, $27.4\sigma_\theta$, and $27.5\sigma_\theta$ to identify the isopycnal pathways and their possible contribution to SPMWs. (In the companion paper [Brambilla *et al.*, 2008], we present a quantitative discussion.)

[56] The hypothesis that cyclonic flow could play an important role in along-isopycnal advection is suggested by the shear that exists between the surface circulation and the circulation on the $27.5\sigma_\theta$ isopycnal [Bower *et al.*, 2002]. While the sea surface is dominated by northeastward flow, the $27.5\sigma_\theta$ isopycnal is characterized by a cyclonic path, with less apparent northeastward flow, that could provide water to the SPMW on the Reykjanes Ridge.

[57] As mentioned in Appendix A, because of the good spatial distribution of the surface drifters, we used them as the primary reference velocity for stream functions on underlying isopycnals (Figure 13, left). The isopycnal stream functions thus obtained are then compared with the absolute stream function computed using the $27.5\sigma_\theta$ floats

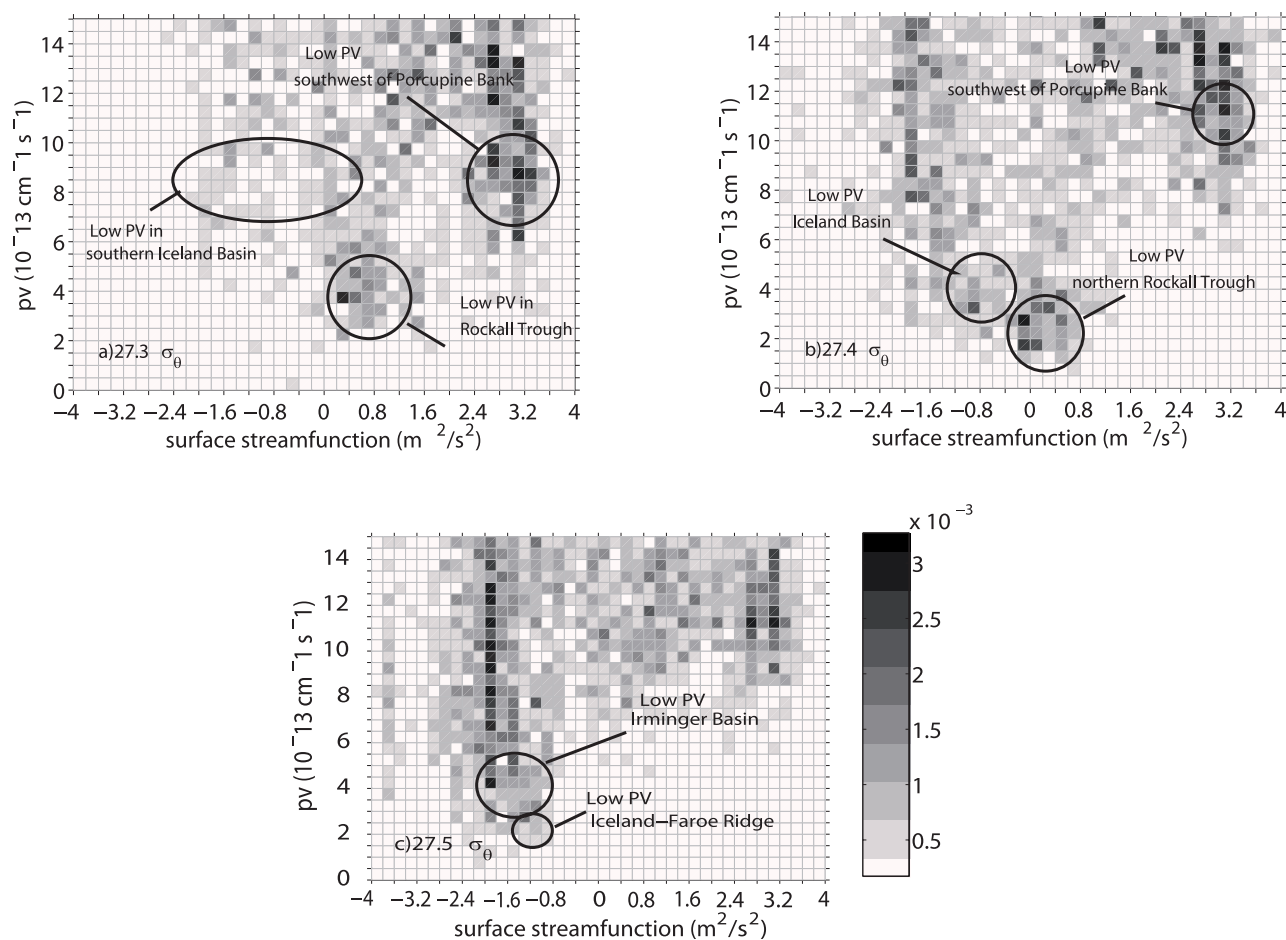


Figure 12. Joint probability density function (pdf) between the surface stream function and the potential vorticity values. The results are shown for a smaller domain than the actual computation domain, in order to focus on the lowest values of potential vorticity. (a) PV at $27.3\sigma_\theta$; (b) PV at $27.4\sigma_\theta$; and (c) PV at $27.5\sigma_\theta$.

as the reference velocity, noting that they have much less spatial coverage than the drifters (Figure 13, right).

[58] The circulation at $27.3\sigma_\theta$ relative to the surface drifters (Figure 13a) is mostly northeastward, resembling the surface circulation since this isopycnal is quite shallow. The northeastward Rockall Trough and Subarctic Front branches of the NAC, where the $27.3\sigma_\theta$ SPMW is present, are well represented. The Central Iceland Basin branch of the NAC is just partially represented because of the nearby outcropping of this isopycnal. The stream function at $27.3\sigma_\theta$ referenced to the $27.5\sigma_\theta$ floats (Figure 13b) does not show an evident separation between the Subarctic Front and the Central Iceland Basin branch of the NAC, probably due to coarse spatial distribution of the floats that requires large smoothing.

[59] The stream function at $27.4\sigma_\theta$ relative to surface drifters (Figure 13c) tracks the Rockall Trough branch of the NAC, the Subarctic Front and the Central Iceland Basin branch of the NAC that partially veers toward the Iceland-Faroe Ridge. The absence of streamlines on the Rockall Plateau is due to intersection of this isopycnal with this topographic feature. Streamlines appear also in the Irminger Sea. One continuous streamline runs cyclonically, connecting the western flank of the Rockall Plateau to the eastern

flank of the Reykjanes Ridge. The flow represented by the stream function at the $27.4\sigma_\theta$ referenced to the $27.5\sigma_\theta$ floats (Figure 13d) does not represent the Rockall Trough branch of the NAC, owing to lack of floats in this area. Moreover, similar to the stream function at the $27.3\sigma_\theta$, the separation between the Subarctic Front and the Central Iceland Basin branch of the NAC is not shown.

[60] On the $27.5\sigma_\theta$ surface (Figure 13e), the connection between the Rockall Trough and the Iceland Basin of the NAC with the Iceland-Faroe Front is less evident, while the cyclonic circulation in the Iceland Basin is more clearly represented. As at $27.4\sigma_\theta$ the stream function computed directly from the $27.5\sigma_\theta$ floats (Figure 13f) is smoother than the stream function referenced to surface drifters. The flow in the Iceland Basin is uniformly northeastward, without distinction between the Subarctic Front and the Central Iceland Basin branch of the NAC.

[61] The depth of the $27.5\sigma_\theta$ isopycnal is large in the center of the Iceland Basin, shoaling westward toward the Reykjanes Ridge. On the Reykjanes Ridge, this isopycnal is shallower than the depth of the remnant winter mixed layer (Figure 3a), suggesting that the $27.5\sigma_\theta$ outcrops in this region. Thus along-isopycnal flow appears to be important for the $27.5\sigma_\theta$ SPMW on the Reykjanes Ridge, reinforcing,

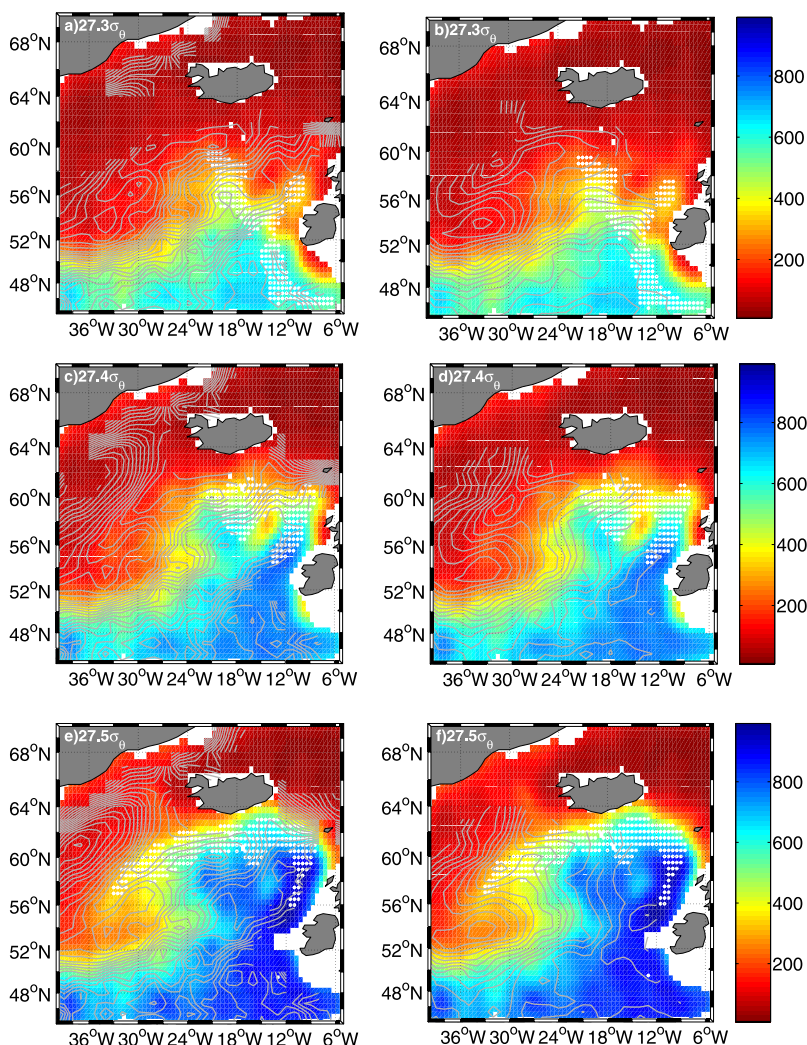


Figure 13. Absolute stream function (gray contour, $\text{m}^2 \text{s}^{-2}$) at: (a, b) $27.3\sigma_\theta$; (c, d) $27.4\sigma_\theta$; and (e, f) $27.5\sigma_\theta$. On each plot the background is the depth (meters) of the corresponding isopycnal. White dots correspond to the location of the SPMW identified as low potential vorticity. In the left plots, the absolute stream function is the pressure anomaly stream function computed with respect to the surface drifter stream function; in the right plots, the absolute stream function is the pressure anomaly stream function computed with respect to the $27.5\sigma_\theta$ float stream function.

at depth, the connection between the Central Iceland Basin branch of the NAC and the East Reykjanes Ridge Current. Isopycnal advection can be as important as diapycnal [McCartney and Talley, 1982] for understanding the origins of SPMW [Brambilla et al., 2008].

6. Summary and Conclusions

[62] In this first part of our two-part study of eastern North Atlantic Subpolar Mode Waters, we focused on properties, relation to the winter mixed layer, locations, and links with the major currents, including various branches of the NAC. We conclude that (1) SPMWs are surface water masses confined between the ocean surface and the permanent pycnocline; (2) SPMWs can be associated with each of the several branches of the NAC in the eastern subpolar gyre; (3) the NAC branches of the northeastern Atlantic do not create a cyclonic pathway connect-

ing the lightest to the densest SPMW, in contrast to the hypothesis of McCartney and Talley [1982]; (4) SPMWs associated with each current branch continuously increase in density downstream; and (5) properties of the $27.5\sigma_\theta$ SPMW on the Reykjanes Ridge differ from those of the $27.5\sigma_\theta$ SPMW on the Iceland-Faroe Ridge. This Reykjanes Ridge SPMW is most likely fed by the western side of the Central Iceland Basin branch of the NAC, that flows northeastward and westward in the Iceland Basin, separate from the Subarctic Front that feeds the Iceland-Faroe Ridge SPMW.

[63] With respect to the first conclusion, SPMWs in the eastern subpolar gyre remain within the remnant of the winter mixed layer, unlike STMW which is subducted into the interior [Hanawa and Talley, 2001]. This is expected because of the general wind-driven upwelling in the subpolar gyre and downwelling in the subtropical gyre. Since in the companion paper [Brambilla et al., 2008] the subpolar

gyre appears to be a region of water mass “subduction” as estimated from convergence of diapycnal volume flux, it is useful to state this basic observation of the vertical distribution of SPMW.

[64] With respect to the second conclusion, identifying SPMW with the minimum of PV, the regions of the eastern subpolar gyre where SPMW is present (Rockall Plateau, southern Iceland-Faroe Ridge, northwestern Reykjanes Ridge) and absent (NAC, northern side of the Iceland-Faroe Front, East Greenland Current) have been located. On isopycnals that intersect the eastern SPMWs ($27.3\sigma_\theta$, $27.4\sigma_\theta$, and $27.5\sigma_\theta$), the absolute stream function and potential vorticity field show how SPMWs are associated with the subpolar gyre currents. (SPMW is not present at the actual property front associated with the currents, but just next to it [Talley, 1999].)

[65] A primary conclusion is that SPMWs are not distributed along a cyclonic flow around the subpolar gyre but instead proceed mainly northeastward, following the predominant direction of the surface flow in the Iceland Basin and Rockall Trough. The northeastward flow in the Iceland Basin consists of two separate branches: the Subarctic Front on the western flank of the Rockall Plateau, and the Central Iceland Basin branch of the NAC that is parallel to the front up to 61°N and then partially veers westward to join the East Reykjanes Ridge Current.

[66] Each of the several branches of the NAC is characterized by SPMW with density increasing smoothly downstream. Along the Subarctic Front and the Rockall Trough branch of the NAC, a progression from $27.3\sigma_\theta$ SPMW to $27.4\sigma_\theta$ SPMW and then $27.5\sigma_\theta$ is found, ultimately feeding the SPMW on the southern side of the Iceland-Faroe Front. The western side of the Central Iceland Basin branch of the NAC is interpreted as the connection between the NAC and the $27.5\sigma_\theta$ SPMW on the Reykjanes Ridge. The Central Iceland Basin branch of the NAC, being separated from the Subarctic Front which acts as a barrier between the eastern and western SPMWs of the Iceland Basin, might also explain the different properties that characterize the $27.5\sigma_\theta$ SPMW on the Reykjanes Ridge and on the Iceland-Faroe Ridge.

[67] In addition, the isopycnal stream functions show that the subsurface flow becomes increasingly cyclonic as density increases from $27.3\sigma_\theta$ to $27.5\sigma_\theta$, in agreement with Bower *et al.* [2002]. Hence along-isopycnal subsurface circulation could be important in connecting subsurface water from the Iceland Basin to the $27.5\sigma_\theta$ SPMW on the Reykjanes Ridge (M. S. McCartney, personal communication, 2006). A detailed discussion of the transformation and formation of SPMWs that addresses this and other issues is presented in the companion paper [Brambilla *et al.*, 2008].

Appendix A: Computation of Absolute Stream Functions

[68] A nondivergent surface stream function is computed from surface drifter velocities [Niiler *et al.*, 2003]. Hydrographic data from WOA01 is then used to compute the stream function on the $27.3\sigma_\theta$, $27.4\sigma_\theta$ and $27.5\sigma_\theta$ isopycnals, using the surface drifter stream function as a reference. An independent reference stream function is also calculated using the $27.5\sigma_\theta$ isopycnal floats [Bower *et al.*,

2002]. The stream function computation follows the objective mapping techniques described by Bretherton *et al.* [1976], Davis [1998, 2005], and Gille [2003].

[69] To obtain an estimate of the geostrophic surface mean velocity field, the Ekman component is first removed from the drifter velocities using the Ralph and Niiler [1999] model [Flatau *et al.*, 2003; Brambilla and Talley, 2006]. The surface drifter velocities are then bin-averaged to form a mean, as in work by Brambilla and Talley [2006]. The entire data set has been used with no correction for time variability. Our surface drifter mean velocity field is similar to Niiler *et al.*'s [2003] adjusted geostrophic stream function based on the same drifters. The reduced smoothing used by Brambilla and Talley, 2006] compared with Niiler *et al.* [2003] is useful to describe the circulation around the Reykjanes Ridge (section 5.1). From the computation of the mean velocity field, we calculate the stream function ψ using a covariance function $C(\rho) = \langle \psi(x, y)\psi(x+r, y+s) \rangle$ that has been assumed to be a priori

$$C(\rho) = \left[1 + \frac{d}{d_0} \right] e^{\left(-\frac{d}{d_0} \right)}, \quad (\text{A1})$$

where d is the radial distance, $d^2 = r^2 + s^2$. The parameter d_0 has been chosen to be 100 km.

[70] The absolute stream functions on the $27.3\sigma_\theta$, $27.4\sigma_\theta$ and $27.5\sigma_\theta$ isopycnal surfaces are obtained by computing the pressure anomaly stream function [Zhang and Hogg, 1992; Gille, 1997] with respect to the ocean surface and then adding the surface stream function values estimated from the surface drifters. The pressure anomaly stream function ψ_1 on the isopycnal surface σ_1 with respect to ψ_2 on the isobaric surface p_2 is

$$\psi_1 - \psi_2 = \int_{p_1}^{p_2} \delta dp - \delta_1 p'_1, \quad (\text{A2})$$

where \bar{p}_1 is the mean pressure of the isopycnal surface, $p'_1 = p_1 - \bar{p}_1$ is the pressure anomaly with respect to the mean pressure on the isopycnal surface, p_2 is the pressure of the isobaric reference surface and δ_1 is the specific volume anomaly or steric anomaly defined by

$$\delta = \frac{1}{\rho(S, T, p)} - \frac{1}{\rho(\bar{S}, \bar{T}, p)}, \quad (\text{A3})$$

where \bar{S} and \bar{T} are the mean salinity and temperature on the reference isopycnal surface, and ρ is the in situ density. The absolute stream function on isopycnal surfaces is the sum of (A2) and the surface stream function estimate ψ_{15m} from surface drifters,

$$\psi_\sigma = \int_{p_1}^{p_2} \delta dp - \delta_1 p'_1 + \psi_{15m}. \quad (\text{A4})$$

[71] It can be argued that the surface drifters are not the proper tool to measure and reference the geostrophic velocity. Although we corrected the drifter velocity measurements by subtracting the Ekman component [Ralph and Niiler, 1999], we cannot exclude the possibility of a residual

ageostrophic velocity and errors related to uncertainties in wind correction [Brambilla and Talley, 2006]. Isopycnal floats, on the other hand, directly measure the geostrophic velocity and can potentially provide a more adequate reference field. In the work by Bower *et al.* [2002], floats were successfully used to calculate the stream function on the $27.5\sigma_\theta$, identified as the geostrophic circulation. However, the float data set has much poorer spatial distribution than the surface drifters in the eastern subpolar gyre [Bower *et al.*, 2002; Brambilla and Talley, 2006]. Hence the absolute stream function from the floats has gaps in some important areas of the SPMW study region, especially in Rockall Trough and over the Iceland-Faroe Ridge, adversely affecting the absolute stream functions at $27.3\sigma_\theta$ and $27.4\sigma_\theta$. Thus their better spatial distribution led us to use the surface drifters as the primary reference. Comparison of the results obtained using the two different reference surfaces in section 5 confirms the validity of our choice.

[72] The procedure to compute the absolute stream function with respect to the $27.5\sigma_\theta$ isopycnal floats is similar to that for the surface drifter reference. First, following Bower *et al.* [2002], the absolute stream function on the $27.5\sigma_\theta$ isopycnal surface was computed from the observed mean velocity field [Davis, 1998; Gille, 2003; Lavender *et al.*, 2005]. Secondly, this mean was used as the reference stream function for the $27.3\sigma_\theta$ and $27.4\sigma_\theta$ isopycnals as in work by Zhang and Hogg [1992],

$$\psi_\sigma = \int_{p_i}^{p_{27.5}'} \delta dp - \delta_i p_i' + \delta_{27.5} p_{27.5}' + \psi_{27.5}, \quad (\text{A5})$$

where $p_{i,27.5}' = p_{i,27.5} - \overline{p_{i,27.5}}$ is the pressure anomaly with respect to the mean pressure on the isopycnal surfaces $\sigma_{i,27.5}$, $\delta_{i,27.5}$ is the specific volume anomaly on the isopycnal surfaces $\sigma_{i,27.5}$, and $\psi_{27.5}$ is the absolute stream function.

[73] **Acknowledgments.** The authors would like to thank S. Gille for useful discussions on objective mapping. This study was supported by the National Science Foundation Ocean Sciences Division, grants OCE-9529584 (WOCE) and OCE-0424893 (CLIVAR). E. Brambilla also received support from the Scripps Institution of Oceanography graduate department.

References

- Arhan, M. (1990), The North Atlantic Current and Subarctic Intermediate Water, *J. Mar. Res.*, *48*, 109–144.
- Bersch, M. (1995), On the circulation of the northeastern North Atlantic, *Deep Sea Res., Part I*, *42*, 1583–1607.
- Bower, A. S., B. Le Cann, T. Rossby, W. Zenk, J. Gould, K. Speer, P. L. Richardson, M. D. Prater, and H.-M. Zhang (2002), Directly measured mid-depth circulation in the northeastern North Atlantic Ocean, *Nature*, *419*, 603–607.
- Brambilla, E., and L. D. Talley (2006), Surface drifter exchange between the North Atlantic subtropical and subpolar gyres, *J. Geophys. Res.*, *111*, C07026, doi:10.1029/2005JC003146.
- Brambilla, E., L. D. Talley, and P. E. Robbins (2008), Subpolar Mode Water in the northeastern Atlantic: 2. Transformation and formation, *J. Geophys. Res.*, *113*, C04025, doi:10.1029/2006JC004063.
- Bretherton, F. P., R. D. Davis, and C. B. Fandry (1976), A technique for objective analysis and design of oceanographic experiments applied to MODE-73, *Deep Sea Res.*, *23*, 559–582.
- Bubnov, V. A. (1968), Intermediate Subarctic Waters in the northern part of the Atlantic Ocean (Engl. transl.), *Okeanologia*, *19*, 136–153. (English translation, *NOO Trans 545*, U.S. Nav. Oceanogr. Off., Washington, D. C., 1973.)
- Conkright, M. E., et al. (2002), *World Ocean Database 2001*, vol. 1, *Introduction*, NOAA Atlas NESDIS, vol. 42, 167 pp., NOAA, Silver Spring, Md.
- Davis, R. (1998), Preliminary results from directly measuring middepth circulation in the tropical and South Pacific, *J. Geophys. Res.*, *103*, 24,619–24,639.
- Davis, R. (2005), Intermediate-depth circulation of the Indian and South Pacific oceans measured by autonomous floats, *J. Phys. Oceanogr.*, *35*, 683–707.
- de Boyer Montégut, C., G. Madec, A. Fisher, A. Lazar, and D. Iudicone (2004), Mixed layer depth over the global ocean: An examination of profile data and profile based climatology, *J. Geophys. Res.*, *109*, C12003, doi:10.1029/2004JC002378.
- Flatau, M. K., L. D. Talley, and P. P. Niiler (2003), The North Atlantic Oscillation, surface current velocities and SST changes in the subpolar North Atlantic, *J. Clim.*, *16*, 2355–2369.
- Fratantoni, D. M. (2001), North Atlantic surface circulation during the 1990s observed with satellite-tracked drifters, *J. Geophys. Res.*, *106*(C10), 22,067–22,093.
- Gille, S. T. (1997), Why potential vorticity is not conserved along mean streamlines in a numerical Southern Ocean, *J. Phys. Oceanogr.*, *27*, 1286–1299.
- Gille, S. T. (2003), Float observations of the Southern Ocean. Part I: Estimating mean fields, bottom velocities, and topographic steering, *J. Phys. Oceanogr.*, *33*, 1167–1181.
- Hanawa, K., and L. D. Talley (2001), Mode waters, in *Ocean Circulation and Climate—Observing and Modelling the Global Ocean*, edited by G. Siedler, J. Church, and J. Gould, pp. 372–386, Academic Press, San Diego, Calif.
- Harvey, J., and M. Arhan (1988), The water masses of the central North Atlantic in 1983–84, *J. Phys. Oceanogr.*, *18*, 1855–1875.
- Kara, A. B., P. A. Rochford, and H. E. Hurlburt (2003), Mixed layer depth variability over the global ocean, *J. Geophys. Res.*, *108*(C3), 3079, doi:10.1029/2000JC000736.
- Kwon, Y.-O., and S. Riser (2004), North Atlantic Subtropical Mode Water: A history of ocean-atmosphere interaction 1961–2000, *Geophys. Res. Lett.*, *31*, L19307, doi:10.1029/2004GL021116.
- Lavender, K. L., W. B. Owens, and R. E. Davis (2005), The mid-depth circulation of the subpolar North Atlantic Ocean as measured by surface floats, *Deep Sea Res., Part I*, *52*, 767–785.
- Marshall, J., D. Jamous, and J. Nilsson (1999), Reconciling thermodynamic and dynamic methods of computation of water-mass transformation rates, *Deep Sea Res., Part I*, *46*, 545–572.
- Masuzawa, J. (1969), Subtropical mode water, *Deep Sea Res.*, *16*, 463–471.
- McCartney, M. S. (1982), The subtropical recirculation of Mode Water, *J. Mar. Res.*, *40*, 427–464.
- McCartney, M. S., and C. Mauritzen (2001), On the origin of the warm inflow to the Nordic Seas, *Prog. Oceanogr.*, *51*, 125–214.
- McCartney, M. S., and L. D. Talley (1982), The Subpolar Mode Water of the North Atlantic, *J. Phys. Oceanogr.*, *12*, 1169–1188.
- McCartney, M. S., and L. D. Talley (1984), Warm-to-cold water conversion in the northern North Atlantic, *J. Phys. Oceanogr.*, *14*, 922–935.
- McClean, J. L., P.-M. Poulain, J. W. Pelton, and M. E. Maltrud (2002), Eulerian and Lagrangian statistics from surface drifters and a high-resolution POP simulation in the North Atlantic, *J. Phys. Oceanogr.*, *32*, 2472–2491.
- Niiler, P. P., N. A. Maximenko, and J. C. McWilliams (2003), Dynamically balanced absolute sea level of the global ocean derived from near-surface velocity observations, *Geophys. Res. Lett.*, *30*(22), 2164, doi:10.1029/2003GL018628.
- Orvik, K. A., and P. Niiler (2002), Major pathways of Atlantic water in the northern North Atlantic and Nordic Seas toward Arctic, *Geophys. Res. Lett.*, *29*(19), 1896, doi:10.1029/2002GL015002.
- Orvik, K. A., and Ø. Skagseth (2003), The impact of the wind stress curl in the North Atlantic on the Atlantic inflow to the Norwegian Sea toward the Arctic, *Geophys. Res. Lett.*, *30*(17), 1884, doi:10.1029/2003GL017932.
- Perez-Brunius, P., T. Rossby, and D. R. Watts (2004), Transformation of the warm waters of the North Atlantic from a geostrophic streamfunction perspective, *J. Phys. Oceanogr.*, *34*, 2238–2256.
- Pickart, R., F. Straneo, and G. W. K. Moore (2003), Is Labrador Sea Water formed in the Irminger Sea?, *Deep Sea Res., Part I*, *50*, 23–52.
- Pollard, R. T., J. F. Read, N. P. Holliday, and H. Leach (2004), Water masses and circulation pathways through the Iceland Basin during Vivaldi 1996, *J. Geophys. Res.*, *109*, C04004, doi:10.1029/2003JC002067.
- Qiu, B., and R. X. Huang (1995), Ventilation of the North Atlantic and North Pacific: Subduction versus obduction, *J. Phys. Oceanogr.*, *8*, 2374–2390.
- Ralph, E., and P. P. Niiler (1999), Wind-driven currents in the tropical Pacific, *J. Phys. Oceanogr.*, *29*, 2121–2129.

- Read, J. F. (2001), CONVEX-91: Water masses and circulation of the northeast Atlantic subpolar gyre, *Prog. Oceanogr.*, *48*, 461–510.
- Reverdin, G., P. P. Niiler, and H. Valdimarsson (2003), North Atlantic Ocean surface currents, *J. Geophys. Res.*, *108*(C1), 3002, doi:10.1029/2001JC001020.
- Rosby, T. (1996), The North Atlantic Current and surrounding waters: At the crossroads, *Rev. Geophys.*, *34*, 463–481.
- Rosby, T., D. Dorson, and J. Fontaine (1986), The RAFOS system, *J. Atmos. Oceanic Technol.*, *3*, 672–679.
- Schmitz, W. J., and M. S. McCartney (1993), On the North Atlantic circulation, *Rev. Geophys.*, *31*, 29–49.
- Speer, K., and E. Tziperman (1992), Rates of water mass formation in the North Atlantic Ocean, *J. Phys. Oceanogr.*, *22*, 93–104.
- Sy, A. (1988), Investigation of large-scale circulation patterns in the central North Atlantic: The North Atlantic Current, the Azores Current, and the Mediterranean Water plume in the area of the Mid-Atlantic Ridge, *Deep Sea Res.*, *35*, 383–413.
- Talley, L. D. (1999), Mode waters in the subpolar North Atlantic in historical data and during the WOCE period, *WOCE Newsl.*, *37*, 3–6.
- Talley, L. D. (2003), Shallow, intermediate, and deep overturning components of the global heat budget, *J. Phys. Oceanogr.*, *33*, 530–559.
- Talley, L. D., and M. S. McCartney (1982), Distribution and circulation of Labrador Sea Water, *J. Phys. Oceanogr.*, *12*, 1189–1205.
- Worthington, L. V. (1976), On the North Atlantic circulation, *Johns Hopkins Oceanogr. Stud.*, *6*, 110 pp.
- Zhang, H., and N. G. Hogg (1992), Circulation and water mass balance in the Brazil Basin, *J. Mar. Res.*, *50*, 385–420.

E. Brambilla and L. D. Talley, Scripps Institution of Oceanography, University of California, San Diego, 9500 Gilman Drive, La Jolla, CA 92093-0208, USA. (elena.brambilla@gm.univ-montp2.fr)